Journal of Catalysis 266 (2009) 218–227

Contents lists available at ScienceDirect

Journal of Catalysis

journal homepage: www.elsevier.com/locate/jcat

Stability and performance of supported Fe–V-oxide catalysts in methanol oxidation

Robert Häggblad, Mariano Massa, Arne Andersson *

Department of Chemical Engineering, Lund University, Chemical Center, P.O. Box 124, SE-221 00 Lund, Sweden

ARTICLE INFO

Article history:
Received 8 June 2009
Revised 10 June 2009
Accepted 11 June 2009
Available online 16 July 2009

Keywords:
Selective oxidation
Methanol
Formaldehyde
Supported Fe–V-oxide
α-Al_2O_3
SiO_2
TiO_2
XRD
XPS
XANES
Volatility

ABSTRACT

As the commercial Fe–Mo-oxide catalyst that is used for oxidation of methanol to formaldehyde suffers from deactivation by Mo volatilization, alternative catalysts are of interest. Therefore, TiO_2-, α-Al_2O_3- and SiO_2-supported (Fe)–V–O catalysts were prepared with a loading of up to 30 μmol of each metal per m^2 surface area of the support. The samples were tested for activity using a high inlet concentration of methanol (10 vol.%), and were characterized by X-ray diffraction (XRD), X-ray photoelectron spectroscopy (XPS) and X-ray absorption spectroscopy (XANES). The activity measurements show that the preparations with the highest loads of V give the best performance. With regard to the support, the activity of the supported catalysts decreases in the order $TiO_2 > Al_2O_3 > SiO_2$. According to XPS, the surface concentration of V decreases in the same order, confirming that vanadium is an active element. At high methanol conversion, the selectivity to formaldehyde decreases from 90% to 80% in the sequence unsupported $FeVO_4 > (Fe)VO_x/TiO_2 \approx (Fe)VO_x/Al_2O_3 > FeVO_x/SiO_2 > VO_x/SiO_2$. Iron has only a small effect on the catalytic performance, whereas it has a stabilizing effect on vanadium decreasing its volatility. However, volatilization experiments reveal that the volatilization of V from the supported (Fe)–V-oxide is much severer than that from bulk $FeVO_4$ due to the dispersion and the comparatively low amount of active metal. Our data demonstrate that neither supported V-oxide nor supported Fe–V-oxide is suitable as a catalyst in the industrial scale production of formaldehyde by methanol oxidation.

1. Introduction

Production of formaldehyde from methanol and air is done with either methanol-rich (36% to 40%) or methanol-lean (8.5% to 9.5%) feed using the silver process and the oxide process, respectively. Historically, the silver process has been preferred over the oxide process mainly due to lower investment costs [1,2], but since the methanol price has almost been doubled over the last five years [3] the more selective oxide process has been favoured considerably. For new formaldehyde capacities, the oxide process is the most common choice today [1,2].

The commercial $MoO_3/Fe_2(MoO_4)_3$ catalyst used in the oxide process is in many aspects superb, showing very high selectivity (~93%) at almost complete conversion of methanol. However, at the reaction conditions the molybdenum is volatile, resulting in lowered activity and poorer selectivity of the catalyst with time on stream as well as increased pressure drop over the catalytic bed [4–8]. Owing to the deactivation, the catalyst has to be replaced every 1 to 2 years depending on the operating conditions [7]. Higher temperature and methanol partial pressure favour the molybdenum loss [8], making it difficult to increase the plant capacity by increasing the methanol concentration. Since the far largest production cost is that of methanol, alternative more stable catalysts are of interest provided that they show comparable selectivity to formaldehyde.

Several vanadates, supported and bulk phases, have been reported promising for methanol oxidation, showing selectivities to formaldehyde above 90% at high methanol conversion [9–21]. However, since vanadium is toxic and because of increasing environmental concerns, low vanadium volatility is desirable not only to improve the catalyst life time, but also to minimize the spread of V inside the plant and in nature. Use of supported vanadium catalysts with loads in the monolayer range can be one approach both to decrease the amount of toxic vanadium being used and to improve the stability of the vanadium through its interaction with the support. In our previous work [20], we characterized and demonstrated that bulk $FeVO_4$ is selective to formaldehyde formation (~90%) at high methanol conversion. To further develop the catalyst with regard to the stability and environmental issues, making it more interesting from a commercial point of view, in the present study we have prepared α-Al_2O_3-, SiO_2- and TiO_2-supported Fe–V–O and V–O catalysts with a load of active material corresponding to 0.5, 1.0, 2.5 and 5.0 theoretical metal oxide layers. The catalysts have been tested for methanol oxidation, and characterized with X-ray diffraction (XRD), X-ray photoelectron spectroscopy (XPS) and XANES (X-ray absorption near edge structure) both before and after 16 h on stream. Further, to investigate the volatility of

* Corresponding author. Fax: +46 46 149156.
E-mail address: Arne.Andersson@chemeng.lth.se (A. Andersson).

0021-9517/$ - see front matter © 2009 Elsevier Inc. All rights reserved.
doi:10.1016/j.jcat.2009.06.010

the vanadium, the V-loss after 5 days of use in methanol oxidation was determined by ICP analysis of the samples, and was compared with the corresponding data for a commercial $MoO_3/Fe_2(MoO_4)_3$-type catalyst. Methanol oxidation was performed with the high methanol inlet composition that today is used in the industry with 10 vol.% methanol and 10 vol.% oxygen, where the oxygen concentration is limited by the lower explosion limit. Moreover, supports with relatively low surface areas were selected considering that the surface area of commercial catalysts often is in the range 4 to 8 m^2/g to limit heat and mass transfer effects, which may cause further oxidation of methanol and formaldehyde to give carbon oxides and thus decreased selectivity [7].

2. Experimental

2.1. Catalyst preparation

α-Al_2O_3-, SiO_2- and TiO_2(anatase)-supported (Fe)–V–O-catalysts were prepared by incipient wetness impregnation of the supports. For each support, four catalysts were prepared with a load of active material corresponding to 0.5, 1.0 and 5.0 theoretical layers of Fe–V-oxide (Fe:V = 1:1) and 2.5 layers of vanadia, respectively. A monolayer is defined as a load of oxide corresponding to 12 μmol cations/m^2 surface area or 7.22 cations/nm^2 [22]. A 0.04 M NH_4VO_3 (Merck) solution and a 0.5 M solution of $Fe(NO_3)_3{\cdot}9H_2O$ (Merck) were prepared separately. Appropriate portions of the two solutions were then mixed together and homogenized by lowering the pH to 1.0 by adding 3 M HNO_3, producing a clear solution with equimolar amounts of vanadium and iron. Using the solution, the α-Al_2O_3, SiO_2 and TiO_2 supports in the form of 0.250 to 0.425 mm particles with specific surface areas of 4.8, 25 and 4.5 m^2/g, respectively, were impregnated by incipient wetness and were dried repeatedly until the desired load of active material was obtained. The intermediate dryings were performed in air at 90 °C for 30 min, and after the final impregnation the drying time was extended to 150 min. Eventually, the catalysts were calcined in air for 6 h at 580 °C. The calcination temperature was selected considering our previous results that 580 °C is required to produce the pure $FeVO_4$ bulk phase calcining precipitates [20]. Elemental analysis by ICP confirmed that the desired load of V and Fe was obtained. In Table 1, the notations, the compositions and the specific surface areas of the prepared catalysts are given.

2.2. Activity measurements

The prepared catalysts were tested for methanol oxidation in a stainless steel reactor, operating at isothermal conditions and at atmospheric pressure. To obtain isothermal conditions, the reactor was embedded in an aluminium block placed in a tube furnace. The catalyst was heated up to the reaction temperature in a flow of 10 ml/min O_2 and 80 ml/min N_2. When the reaction temperature of 300 °C was reached, a flow of 10 ml/min gaseous methanol was added to the flow of oxygen and nitrogen. Methanol, formaldehyde (FA), dimethyl ether (DME), methyl formate (MF), dimethoxymethane (DMM) and CO_2 were analyzed online using a gas chromatograph equipped with a Haysep C column and both an FID and a TCD detector. CO was analyzed online on an IR instrument (Rosemount Binos 100). All catalysts were run overnight, and the activities obtained after 16 h on stream are presented.

For characterization of the samples with XRD, XPS and XANES after use in methanol oxidation, 0.4 g catalyst was run for 16 h and then cooled under flowing nitrogen. Before the analyses, the sample was mixed thoroughly and ground to powder.

2.3. Catalyst characterization

The specific surface areas of the catalysts were measured on a Micromeritics Flowsorb 2300 instrument. The single point BET method was used with adsorption of nitrogen at liquid nitrogen temperature and subsequent desorption at room temperature. All samples were degassed at 150 °C for 24 h before analysis.

X-ray powder diffraction (XRD) analysis was performed on a Seifert XRD 3000 TT diffractometer using Ni-filtered Cu Kα radiation and a rotating sample holder. Data were collected between 5° and 80° 2θ in steps of 0.1° (2.0 s/step).

XPS analysis was performed on a PHI 5500 XPS instrument using monochromatic Al Kα radiation. Powder samples were placed on a conducting and sticky tape. To minimize the effects of sample charging, the aluminium-containing samples were charge neutralized by electrons. The PC-ACCESS and MuliPak 6.1A softwares were used to evaluate the data, and the quantifications were made using a Shirley function for the background. The C 1s peak was used as an energy reference, and was set to a binding energy of 285.0 eV.

The XANES measurements were performed at the I811 beamline in Maxlab (Lund University) using a Si(1 1 1) double crystal monochromator and three ionization chambers. Spectra of the Fe

Table 1
Notation, composition and specific surface area of the prepared catalysts.

Sample	Support	Active oxide phase			Specific surface area (m^2/g)
		wt.%[a]	No. of layers[b]	V:Fe ratio	
TiO_2					4.5
0.5FeVTi	TiO_2	0.22	0.5	1:1	4.7
1FeVTi	TiO_2	0.46	1.0	1:1	4.7
5FeVTi	TiO_2	2.24	5.0	1:1	4.4
2.5VTi	TiO_2	1.21	2.5	1:0	3.8
α-Al_2O_3					4.8
0.5FeVAl	α-Al_2O_3	0.24	0.5	1:1	5.2
1FeVAl	α-Al_2O_3	0.49	1.0	1:1	5.2
5FeVAl	α-Al_2O_3	2.42	5.0	1:1	5.7
2.5VAl	α-Al_2O_3	1.31	2.5	1:0	5.3
SiO_2					25
0.5FeVSi	SiO_2	1.13	0.5	1:1	22
1FeVSi	SiO_2	2.50	1.0	1:1	26
5FeVSi	SiO_2	11.36	5.0	1:1	25
2.5VSi	SiO_2	6.42	2.5	1:0	21

[a] Expressed as wt.% $FeVO_4$ and V_2O_5, respectively, for the samples with and without iron.
[b] Number of theoretical oxide layers where a layer is defined as a load of oxide with 12 μmol cations/m^2 surface area of the support.

K- and V *K*-edges were recorded in fluorescence mode. The sample was placed after the first ionization chamber and located 45° to both the incoming beam and the fluorescence detector. The detectors used were a five-grid ion chamber Lytle detector for the α-Al_2O_3- and SiO_2-supported catalysts and an energy dispersive Si(Li)-detector for the TiO_2-supported catalysts. Due to overlapping Ti $K\beta_{1,3}$ (4931.8 eV), V $K\alpha_1$ (4952.2 eV) and V $K\alpha_2$ (4944.6 eV) emission lines, the much weaker V $K\beta_{1,3}$ (5427.3 eV) emission line was selected for analysis of the vanadium in the TiO_2-supported catalysts. Unfortunately, the weak signal only allowed recording of XANES spectra for the catalyst with highest load of active phase (5FeVTi). For calibration of the energies, spectra of Fe and V metal foils were recorded online in transmission mode.

To study the volatility of vanadium in methanol oxidation, 0.02 g catalyst was treated for 5 days at 300 °C in a flow of nitrogen with 10% methanol and 10% oxygen. The amount of catalyst was selected to assure differential conversion of methanol (<10%), corresponding to reactor inlet conditions. After the treatment, the catalyst was subjected to elemental analysis with ICP-AES. By comparing the analysis result with that of the corresponding analysis for the as-prepared catalyst, the loss of vanadium due to volatilization was determined. An industrial-type $MoO_3/Fe_2(MoO_4)_3$ catalyst was subjected to the same treatment, giving the volatilization of molybdenum for comparison.

2.4. Reference samples

For comparative purposes a phase pure $FeVO_4$ sample and a commercial-type iron molybdate catalyst are used. The $FeVO_4$ catalyst with the surface area of 15.2 m^2/g has previously been characterized and compared with the molybdate catalyst for methanol oxidation [20]. The iron molybdate sample has a specific surface area of 7.0 m^2/g and a Mo/Fe atomic ratio of 2.4 in the form of two crystalline phases $Fe_2(MoO_4)_3$ and MoO_3.

As a reference compound for XANES, a solid solution $V_xTi_{1-x}O_2$ with $x = 0.15$ was prepared by heating a mixture of V_2O_5 and TiO_2(anatase) powders at 1000 °C until the sample according to XRD was a black single phase solid solution.

3. Results and discussion

3.1. X-ray diffraction

The supported 2.5V and 5FeV catalysts with relatively high loads of active phase were characterized by XRD and were compared with the pure $FeVO_4$ to establish the presence of any crystalline phases in the samples. As seen in Fig. 1, the $FeVO_4$ bulk catalyst shows the characteristic pattern of triclinic ($P\bar{1}$) $FeVO_4$, JCPDS 25-418 [23]. The alumina- and titania-supported samples show only peaks from the supports, α-Al_2O_3 (JCPDS 10-173) [23], respectively, TiO_2 in the form of anatase (JCPDS 21-1272) with some rutile (JCPDS 21-1276) [23]. For the pure TiO_2 support, the contents of anatase and rutile are approximately 91% and 9%, respectively, as obtained from the intensity ratio between the strongest XRD peak from each polymorph using the relationship of Spurr and Myers [24]. After deposition of vanadium, the proportion of rutile increased to 12% and 27% in 5FeVTi and 2.5VTi, respectively, showing that the presence of Fe largely inhibits the phase transition. In the literature, it is well established that the presence of vanadia on anatase accelerates and lowers the temperature for the anatase to rutile phase transition [25–29]. Also it has been found that a $V_xTi_{1-x}O_2$ rutile phase with a small amount of V^{4+} may form [25,26,28].

The fact that no crystalline phases in addition to the support were detected by XRD in the alumina- and titania-supported 2.5V and 5FeV samples with loads exceeding a theoretical monolayer does not exclude the formation of such phases, considering that both the surface area and the consequent vanadium content of the samples are low (Table 1). On the contrary, the XRDs of the silica-supported samples with higher surface areas and vanadium contents, besides amorphous silica, show the formation of additional crystalline phases. In the 5FeVSi sample, α-Fe_2O_3, JCPDS 33-664 [23], and $FeVO_4$ are present, whereas 2.5VSi shows characteristic V_2O_5 peaks, JCPDS 41-1426 [23].

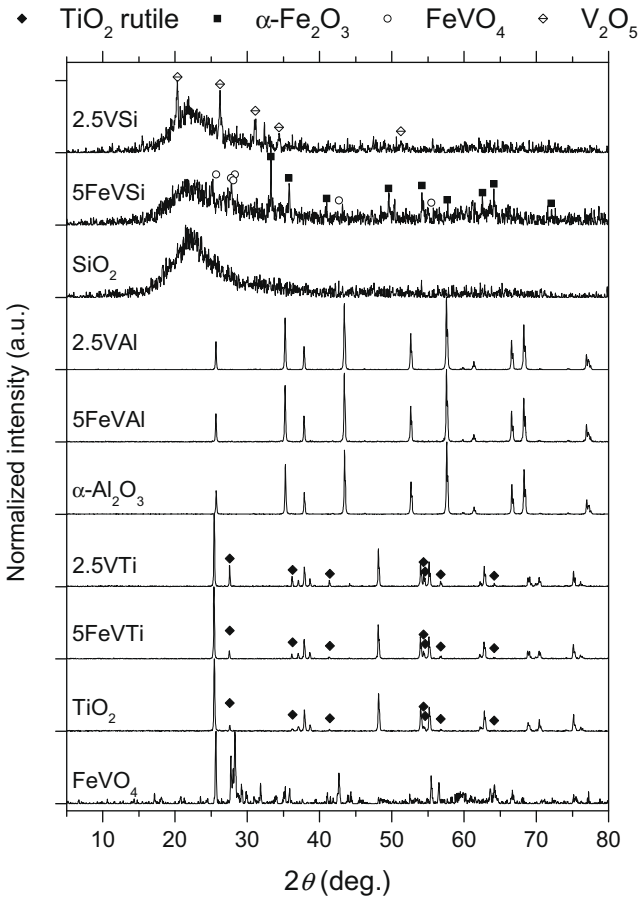

Fig. 1. XRD patterns of as-prepared $FeVO_4$ and supported catalysts with 2.5 monolayers V-oxide and 5.0 monolayers FeV-oxide (Fe:V = 1:1), respectively. The diffractograms of the bare supports TiO_2, α-Al_2O_3 and SiO_2 are included for comparison.

3.2. XPS

XPS measurements were performed on the supported samples to determine the elemental composition and the oxidation states of the elements in the surface region both as synthesized and after use in methanol oxidation. The samples are designated fresh and used, respectively. For fresh samples, the binding energies of $V2p_{3/2}$ and $Fe2p_{3/2}$ are in the 517.0 to 517.8 eV and 711.4 to 712.0 eV range, respectively, and the peaks are symmetric, confirming that vanadium and iron on the fresh catalysts are pentavalent [20,30,31] and trivalent [20,32,33], respectively. The used catalysts supported on TiO_2 and α-Al_2O_3 show reduction of neither vanadium nor iron after methanol oxidation. However, for the used SiO_2-supported 5FeVSi and 2.5VSi catalysts the binding energies of the $V2p_{3/2}$ peak are 516.9 and 516.6 eV, respectively, indicating minor reduction of the vanadium. Considering that the XRD in Fig. 1 is showing the presence of $FeVO_4$ in the fresh 5FeVSi sample, reduction of vanadium but not of iron is in agreement with previous findings for bulk $FeVO_4$ [20].

Considering the dispersion of vanadium and iron as analyzed by XPS, the metal ratios given in Table 2 clearly show that vanadium is considerably better dispersed than iron for all supports, indicating V-support interaction. On TiO_2 and α-Al_2O_3, moreover, the vanadium to support ratios V/S are similar for the fresh 5FeV and 2.5V samples, indicating for the samples with iron formation of dispersed vanadia and separate iron oxide particles or domains rather than of dispersed iron vanadate. In Fig. 2, the V/S ratios are plotted against the number of theoretical layers of vanadium. From the plots for TiO_2, α-Al_2O_3 and SiO_2, the V/S ratios for a load of one monolayer are estimated to be 0.22, 0.10 and 0.06, respectively, revealing that the surface concentration of vanadium on TiO_2 is considerably higher than that on α-Al_2O_3 and SiO_2. Moreover, the linear curve shape below one monolayer coverage suggests that on TiO_2 the V is evenly distributed on the surface. When exceeding a load of one monolayer, the curve slope decreases due to the formation of additional larger vanadia particles in agreement with previous findings [34]. For the alumina-supported samples, the V/Al ratio increases with the vanadium content and tends to a limiting value, which is lower than that for TiO_2. This behaviour suggests the formation of a dispersed $AlVO_4$-type structure as will be explained in more detail in Section 3.4. On SiO_2, however, the linear increase of the V/S ratio up to 2.5 layers of vanadium suggests that the dispersion of vanadium is poor in agreement with mainly crystalline phases being formed (Fig. 1). The poor dispersion of vanadia on SiO_2 has been observed also by others [13,35–37], and has been explained by the low surface concentration of hydroxyl groups [37]. As displayed in Table 2, generally there are only small differences between the respective V/Ti and V/Al ratios before and after 16 h of methanol oxidation, revealing no major changes of the dispersion of vanadium. For SiO_2, however, a considerably lower V/Si ratio is observed after methanol oxidation both at low and high loads of active phase.

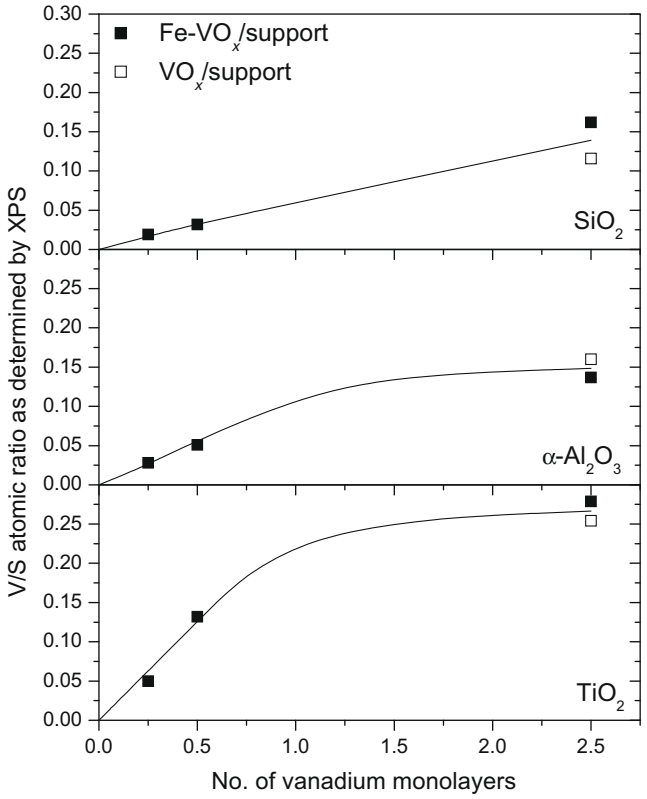

Fig. 2. Vanadium to support atomic ratios (V/S) as a function of the vanadium load for freshly prepared TiO_2-, α-Al_2O_3- and SiO_2-supported catalysts as determined by XPS.

3.3. XANES

As a complement to the XPS data, XANES measurements were carried out to obtain further information about the coordination and the valences of the supported elements.

In Fig. 3, V *K*-edge spectra of the fresh 5FeV catalysts are compared with those of the reference compounds $V_{0.15}(IV)Ti_{0.85}O_2$ rutile phase, $V_2(V)O_5$ and $FeV(V)O_4$, and moreover, fresh and used 5FeV samples are compared. The main edge positions for the fresh 5FeVTi, 5FeVAl and 5FeVSi are 5481.7, 5481.3 and 5481.3 eV, respectively, and for the $V_{0.15}(IV)Ti_{0.85}O_2$, V_2O_5 and $FeVO_4$ reference compounds they are 5476.8, 5480.0 and 5481.5 eV, respectively, revealing that the vanadium is pentavalent in all fresh catalysts. The fact that both XPS and XANES of the fresh 5FeVTi reveal the vanadium to be pentavalent suggests that the rutile phase observed by XRD (Fig. 1) in both 5FeVTi and 2.5VTi is either without V^{4+}, or in the form of a $V_xTi_{1-x}O_2$ solid solution [25,26,28] with only a very small amount of V^{4+}. On the other hand, as displayed in Fig. 3, after 16 h in methanol oxidation the V *K*-edge position of the used 5FeVTi catalyst is shifted 1.7 eV towards lower energy, showing reduction of some vanadium. However, the reduction observed by XANES is not seen in XPS. In contrast to XANES, XPS is more surface-sensitive, and therefore the results suggest that the reduced vanadium is from the bulk. Possibly, during the reaction some V^{4+} is formed dissolving in the TiO_2 rutile phase to form $V_x(IV)Ti_{1-x}O_2$.

Considering both the pre-edge intensity and the post-edge feature, it can be seen in Fig. 3 that the V *K*-edge spectrum for 5FeVTi clearly resembles that for the $V_{0.15}(IV)Ti_{0.85}O_2$ reference when accounting for the energy shift due to the difference in oxidation state. The resemblance suggests a high degree of octahedrally coordinated vanadium to be present in 5FeVTi. However, the somewhat larger pre-peak area (broader and higher) for 5FeVTi indicates that there might also be less coordinated vanadia. It has been demonstrated that on hydrated VO_x/TiO_2 octahedrally coordinated V is common on both rutile and anatase TiO_2 [38–42]. However, after dehydration the predominant coordination is tetrahedral [37,39,40]. A XANES spectrum calculated for a mix of 30% 4-coordinated ($FeVO_4$) and 70% 6-coordinated ($V_{0.15}Ti_{0.85}O_2$) vanadium is presented in Fig. 4, showing a spectrum very similar to that of 5FeVTi. Thus, the XANES results suggest that at ambient conditions a mixture of octahedral and tetrahedral vanadia is present on the non-dehydrated 5FeVTi.

As shown in Fig. 3, after use in methanol oxidation reduction of vanadia is observed for neither 5FeVAl nor 5FeVSi. The 5FeVSi

Table 2
Dispersion of V and Fe on the supports (S) as analyzed by XPS.

Catalyst notation	Fresh catalysts			Used catalysts[a]		
	V/S	Fe/S	V/Fe	V/S	Fe/S	V/Fe
0.5FeVTi	0.050	0.033	1.5	0.055	0.031	1.8
1FeVTi	0.132	0.037	3.6	0.129	0.042	3.1
5FeVTi	0.279	0.054	5.2	0.256	0.039	6.6
2.5VTi	0.254	–	–	0.364	–	–
0.5FeVAl	0.028	0.012	2.3	0.012	0.004	3.0
1FeVAl	0.051	0.030	1.7	0.060	0.034	1.8
5FeVAl	0.137	0.055	2.5	0.130	0.037	3.5
2.5VAl	0.160	–	–	0.152	–	–
0.5FeVSi	0.019	0.001	19.8	0.008	0.001	7.0
1FeVSi	0.032	0.005	6.5	0.013	0.003	3.7
5FeVSi	0.162	0.031	5.2	0.062	0.024	2.6
2.5VSi	0.116	–	–	0.073	–	–

[a] The samples have been used at 300 °C for 16 h in methanol oxidation with 10 vol.% each of methanol and oxygen (see Section 2.2).

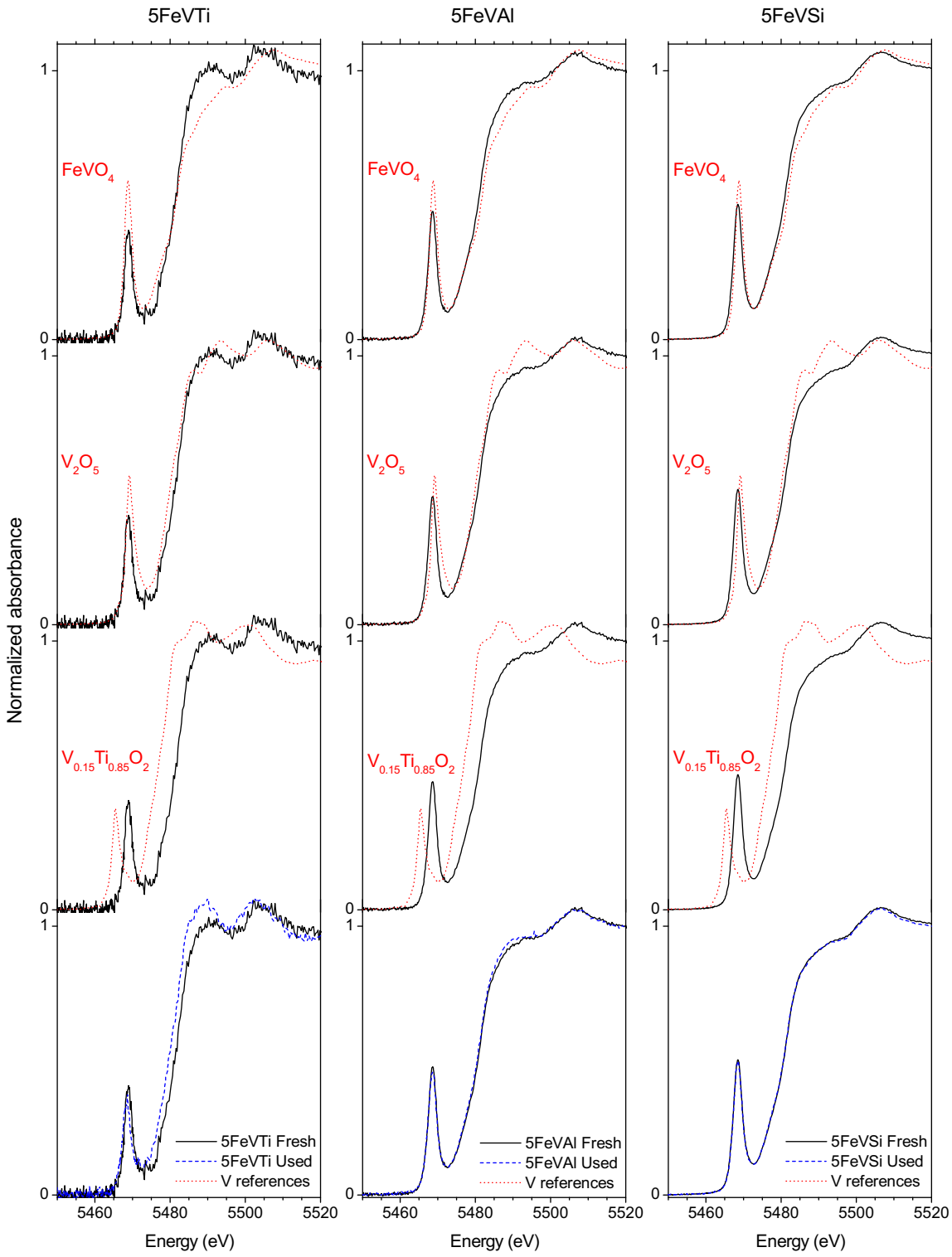

Fig. 3. Normalized V *K*-edge XANES spectra for fresh (solid line) and used (dashed line) 5FeVTi, 5FeVAl and 5FeVSi samples (bottommost) and for fresh 5FeVTi (left column), 5FeVAl (middle column) and 5FeVSi (right column) along with the reference compounds (dotted line) $V_xTi_{1-x}O_2$ rutile with $x = 0.15$, V_2O_5 and $FeVO_4$. The spectra for the used samples were recorded after 16 h of use in methanol oxidation at 300 °C and with 10% methanol and 10% oxygen in nitrogen (see Section 2.2).

spectrum is very similar to the $FeVO_4$ spectrum from tetrahedrally coordinated vanadium, a fact which is in agreement with the XPS and XRD data given in Table 2 and Fig. 1, respectively, showing poor dispersion of vanadia on SiO_2 and formation of $FeVO_4$ and α-Fe_2O_3. However, the pre-edge intensity of the supported catalyst is slightly lower than that observed for $FeVO_4$, suggesting a higher degree of hydrated vanadia on 5FeVSi. At hydrated conditions, vanadia on silica with a high surface area has been reported to be present as polymeric species possessing square pyramidal coordination [43]. Analogous to vanadia on SiO_2, the V *K* XANES spectral feature of 5FeVAl shown in Fig. 3 suggests the formation of a (Fe,Al)VO_4 mixed surface structure due to reaction between α-Al_2O_3, Fe and V [20,44,45]. Our observation that vanadium on α-alumina, like in $FeVO_4$, is in tetrahedral coordination agrees with previous

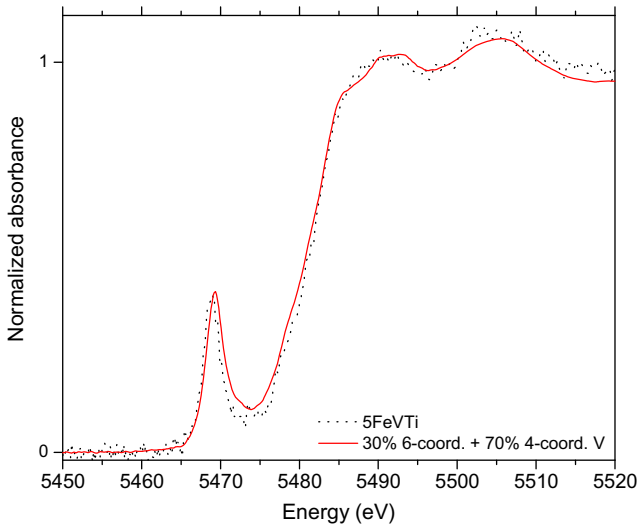

Fig. 4. The normalized V *K*-edge XANES spectrum for the fresh 5FeVTi and a spectrum calculated for a mixture of 70% octahedrally coordinated and 30% tetrahedrally coordinated vanadium as obtained from the spectra for $V_{0.15}Ti_{0.85}O_2$ and $FeVO_4$, respectively. In order to simulate a pentavalent octahedral reference, adjustment of the V *K*-edge position for the tetrahedrally coordinated V^{4+} in $V_{0.15}Ti_{0.85}O_2$ was made (+4.0 eV).

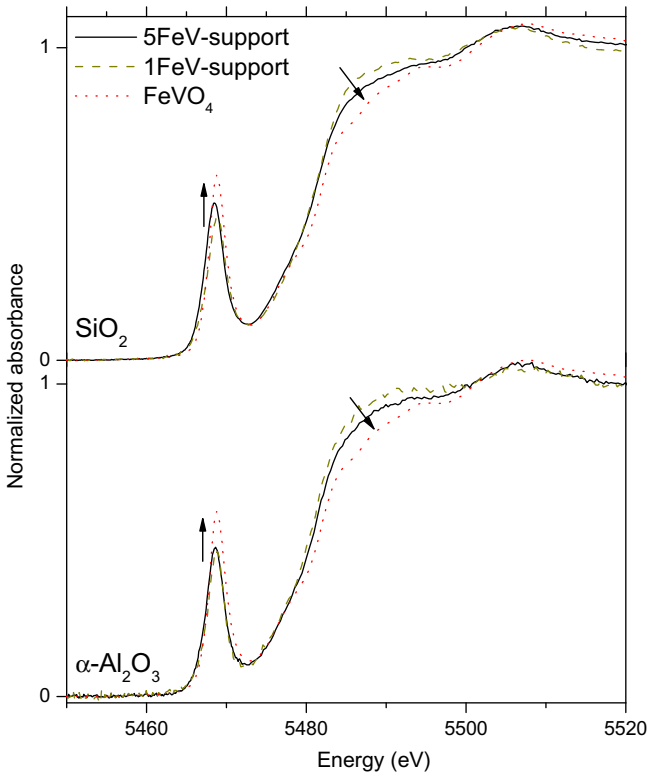

Fig. 5. Normalized V *K*-edge XANES spectra for fresh 1FeVAl, 5FeVAl, 1FeVSi and 5FeVSi and bulk $FeVO_4$. The arrows illustrate the trend when increasing the amount of active phase on the supports.

XANES/EXAFS characterizations of the Fe-free vanadia/γ-alumina system [43,46,47], where both hydrated and dehydrated samples have tetrahedrally coordinated vanadium [46,47].

Concerning the 1FeV samples with lower load of active material, as described in Section 2.3 it was not possible to analyze 1FeVTi. V *K*-edge spectra for the fresh 1FeV and 5FeV on α-Al_2O_3 and SiO_2 are compared in Fig. 5, showing that for both supports the spectrum becomes more similar to that for $FeVO_4$ when the load of active phase is increased. Possibly, the trend is due to a relatively larger fraction of the vanadium being present in hydrated form at a low load.

Fe *K* XANES spectra for the freshly prepared 5FeVTi, 5FeVAl and 5FeVSi are presented in Fig. 6 together with spectra of the Fe^{2+}/Fe^{3+} phase Fe_3O_4 and the Fe^{3+} phases α-Fe_2O_3, γ-Fe_2O_3 and $FeVO_4$. The edge positions indicate that Fe in all catalysts is in its highest oxidation state. Fig. 6 also reveals that in 5FeVTi iron is mainly gathered as particles or domains of α-Fe_2O_3, confirming the XPS results showing poor dispersion of Fe on TiO_2. Also for α-Al_2O_3, the results suggests that α-Fe_2O_3 domains are formed, which is not surprising since both α-Al_2O_3 and α-Fe_2O_3 possess the corundum oxide structure [48]. For 5FeVSi, the spectrum suggests that most iron is present as $FeVO_4$. The fact that the XRD pattern of 5FeVSi shown in Fig. 1 shows stronger peaks from α-Fe_2O_3 than from $FeVO_4$ is in line with our observation that of the pure phases, the former gives the fewest and most intense peaks in XRD.

3.4. Structure activity relationships

The data given in Table 3 for 30% methanol conversion show that the titania-supported FeVTi catalysts, compared with bulk $FeVO_4$, give slightly lower selectivity to formaldehyde and DME, whereas their selectivity to carbon oxides is higher. Moreover, the specific activity increases with the load of vanadium and iron. Considering that XPS gives a V:Fe ratio of 1.5 to 2.0 for $FeVO_4$ [20], the observation that the activity is higher for 5FeVTi than for bulk $FeVO_4$ can be explained by the concentration of active V-sites being higher on 5FeVTi, which is supported by the XPS data given in Table 2 and Fig. 2 showing good dispersion and coverage of V compared to Fe (V:Fe = 5.2). Further support for the latter inference are the activity data given in Table 3 showing similar activity for 5FeVTi and 2.5VTi, and the XPS data given in Table 2 showing similar V/Ti ratios for the samples. Compared with the FeVTi samples and the pure $FeVO_4$, 2.5VTi is less selective to formaldehyde formation (Table 3), indicating a promotional role of iron.

Compared with the titania-supported samples, the corresponding alumina-supported samples are less active (Table 3). According to the XPS data given in Table 2, the lower activity at least partly is related to the lower surface concentration of vanadium on alumina. Concerning the product distribution at low vanadium content (0.5FeVAl and 1FeVAl), it is notable in Table 3 that the selectivity to formaldehyde rapidly decreases with an increase of conversion and that essentially carbon oxides are formed. On the contrary, formaldehyde is the main product on 5FeVAl and 2.5VAl. Considering that vanadium is better dispersed than iron on the alumina samples (Table 2), it is noteworthy that both 1FeVAl and 0.5FeVAl have vanadium loads below the monolayer range, while 5FeVAl and 2.5VAl have loads corresponding by definition to 2.5 theoretical layers of vanadia. The difference in load thus proposes that some more isolated vanadia species or ensembles on alumina give combustion, while the more extended structure formed at higher load of vanadium and iron is much more selective to formaldehyde.

Compared with the V/Ti ratios measured by XPS for the titania-supported samples, the V/Al ratios that the corresponding alumina samples show are approximately only half (Table 2). This composition suggests either the formation of an extended $AlVO_4$-type structure on the alumina support, or dissolution of V^{3+} in the α-Al_2O_3 forming α-$Al_{2-x}V_xO_3$. According to XANES (Fig. 3), the formation of the latter structure is unlikely since the vanadium in the catalyst predominantly is pentavalent. The formation of an $AlVO_4$-type structure is in agreement with the observation that vanadium can react with alumina forming crystalline $AlVO_4$ during

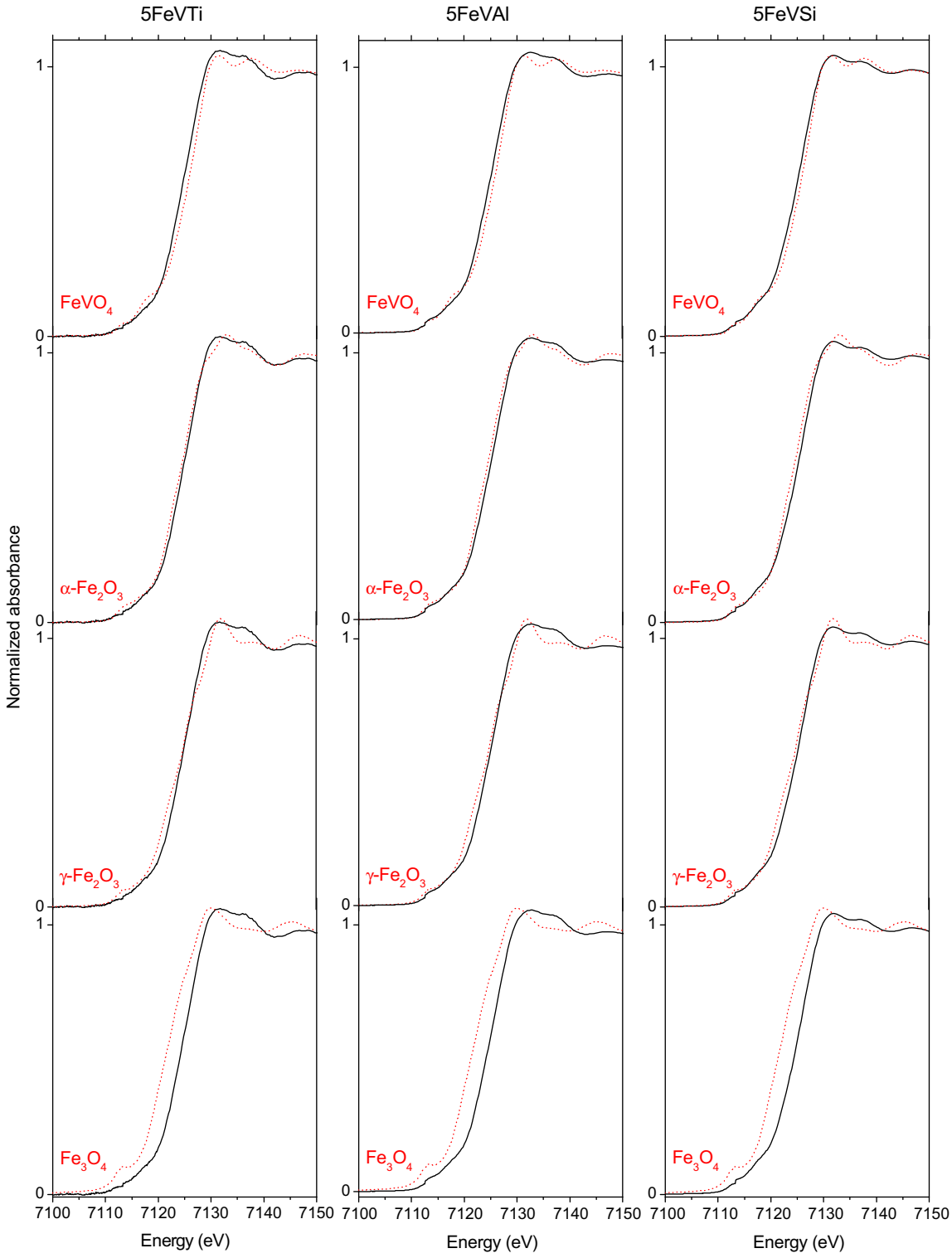

Fig. 6. Normalized Fe *K*-edge XANES spectra for the fresh (solid line) 5FeVTi, 5FeVAl and 5FeVSi catalysts and the reference compounds (dotted line) Fe_3O_4, γ-Fe_2O_3, α-Fe_2O_3 and $FeVO_4$.

calcination at 550 to 600 °C [20,44,45]. Moreover, besides forming iron oxide, some iron may enter the vanadate structure forming $Al_{1-x}Fe_xVO_4$ on the alumina surface. Support for this indication are the activity data given in Table 3, showing that 5FeVAl is less active than $FeVO_4$ and 2.5VAl in agreement with our previous result that $Al_{1-x}Fe_xVO_4$ with both Al and Fe is less active than both end compositions [20].

In contrast to vanadia on γ-alumina producing DME at low vanadia loads and approximately equal amounts of formaldehyde and DME at monolayer coverage [13], our data for vanadate on α-alumina show the formation of predominantly carbon oxides and formaldehyde at low and high loads of vanadium, respectively. Also in a previous investigation it is reported that vanadia on α-alumina is much more selective to formaldehyde than to DME [49].

Table 3
Specific activity and selectivity to products[a] at 30% methanol conversion.

Catalyst	Specific activity (μmol/m^2,s)	Selectivity (%)				
		FA	DME	DMM	MF	CO_x
$FeVO_4$	4.328	86.4	1.5	2.8	5.6	3.7
0.5FeVTi	2.061	84.0	0.7	3.3	5.3	6.7
1FeVTi	2.971	82.5	0.5	2.3	4.9	9.7
5FeVTi	6.336	83.4	0.3	3.8	4.8	7.7
2.5VTi	5.617	79.7	1.3	2.9	6.5	9.6
0.5FeVAl	0.180	49.6[b]	3.0[b]	20.9[b]	10.0[b]	16.6[b]
1FeVAl	0.282	21.8[c]	0.4[c]	1.9[c]	3.4[c]	72.5[c]
5FeVAl	2.836	81.7	0.9	3.3	8.8	5.4
2.5VAl	4.126	81.4	1.2	2.3	8.5	6.6
0.5FeVSi	0.035	73.3	0.8	2.1	12.6	11.2
1FeVSi	0.084	72.3	1.0	1.9	14.4	10.4
5FeVSi	0.149	78.7	1.1	2.2	9.6	8.5
2.5VSi	0.254	76.7	2.8	2.0	12.3	6.2

[a] Formaldehyde (FA), dimethyl ether (DME), dimethoxymethane (DMM), methyl formate (MF) and carbon oxides (CO_x).
[b] 5% conversion.
[c] 20% conversion.

Of the supports used, silica shows the lowest activity to the catalyst in agreement with previous findings [13]. Also in agreement with previous reports, the low activity of the FeVSi samples and 2.5VSi is a consequence of the weak interaction of vanadia with silica [13,35–37], in the present case resulting in the formation of crystalline V_2O_5 in the Fe-free 2.5VSi and $FeVO_4$ when both iron and vanadium are present as shown by the XRDs in Fig. 1. Obviously, these crystalline phases contribute little to the surface area and consequently to the specific activity. According to XPS (Table 2), compared with the V/Al ratios for the alumina-supported samples, the V/Si ratios that the silica-supported samples present are not much lower. However, here we have to consider that on alumina, aluminium enters the active structure spread on the alumina surface, whereas on silica separate non-interacting vanadia crystallites are formed. These crystallites, in contrast to the low activity of the samples, cannot explain the relatively high V/Si ratios observed. Consequently, the V/Si ratios indicate the formation of a limited amount of more or less dispersed vanadia interacting with silica. The formation of such species has been reported in previous studies [13,50–54], and is in agreement with our XRD for 5FeVSi with V:Fe = 1 in Fig. 1 showing the presence of α-Fe_2O_3 and $FeVO_4$ only, indicating the presence of a second vanadia structure. According to Deo and Wachs [13], the interacting species however present very low turnover numbers for methanol oxidation. Concerning our indication that $FeVO_4$ crystallites are the major active species on the FeVSi samples, the results given in Table 3 that bulk $FeVO_4$ is more selective than the FeVSi samples to formaldehyde may be a particle size effect, giving different distributions of surface planes on large and small crystallites, respectively. The fact that 2.5VSi with crystalline V_2O_5 is reasonably selective to formaldehyde is in line with the data for unsupported vanadia [20,55].

The catalytic performances at high methanol conversion of the catalysts with the highest load of active material on each support are displayed in Fig. 7. Here it can be seen that all samples are selective to formaldehyde at high methanol conversion, although as discussed before, the activities differ considerably. The selectivity to formaldehyde varies from 90% to 80%, and decreases in the order bulk $FeVO_4$ > (Fe)$VO_x/TiO_2 \approx$ (Fe)VO_x/Al_2O_3 > $FeVO_x/SiO_2$ > VO_x/SiO_2. Concerning the selectivity to methyl formate, there is clearly an influence from the type of support in that the selectivity increases from 4.5% to 13% in the order unsupported $FeVO_4$ < (Fe)VO_x/TiO_2 < (Fe)VO_x/Al_2O_3 < (Fe)VO_x/SiO_2. Besides methyl formate, other major by-products are carbon oxides, for which there is no clear trend among the supported samples. However, the unsupported $FeVO_4$ shows lower selectivity. In all cases, the amount of DME formed at high methanol conversion is low.

3.5. Volatilization of vanadium

Due to volatilization of molybdenum from commercial iron molybdate catalysts in methanol oxidation [4–8], alternative catalysts are of interest provided that they are more stable. Therefore, it is of interest to quantify the volatility of vanadium from the supported catalysts. Consequently, the V-loss was determined by elemental quantification of the fresh catalysts and the corresponding catalysts treated for 5 days at 300 °C in an atmosphere with 10 vol.% methanol and 10 vol.% O_2 in N_2. Data are presented in Table 4 for the supported catalysts, and for comparison the corresponding data for the unsupported reference samples $FeVO_4$ and an iron molybdate catalyst are also given. There are several obstacles when comparing the volatilization data. For the supported cat-

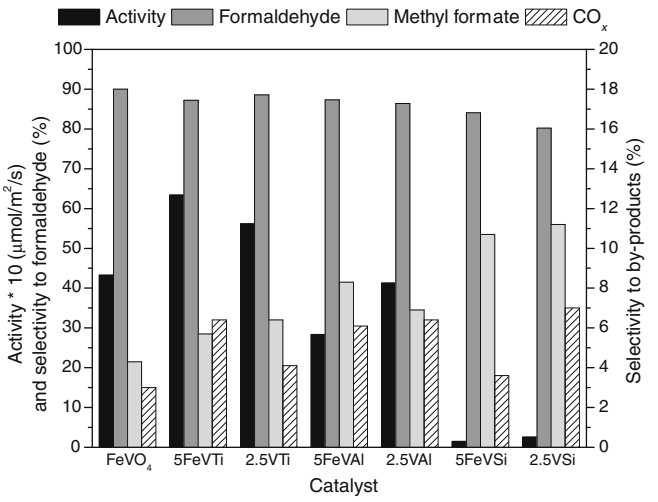

Fig. 7. Catalytic data for TiO_2-, α-Al_2O_3- and SiO_2-supported catalysts with a load of 2.5 theoretical layers of vanadia and either with or without the same load of iron (notations as in Table 1). Corresponding data for $FeVO_4$ are included for comparison. The selectivities to formaldehyde, CO_x and dimethyl ether (DME) are for 80% methanol conversion. For calculation of the specific activity, data for low methanol conversion were used to relate the activity to well-defined partial pressures. Inlet gas composition: 10 vol.% methanol and 10 vol.% oxygen in nitrogen. Temperature: 300 °C.

Table 4
Volatilization of active metals[a] from supported (Fe)–V-oxide, bulk $FeVO_4$ and an iron molybdate catalyst.

Catalyst	Element	Element loss		
		(%)	(mmol/g catalyst)	(mmol/m^2 catalyst)
$MoO_3/Fe_2(MoO_4)_3$	Mo	35.7	1.701	0.242
$FeVO_4$	V	5.7	0.334	0.022
1FeVTi	V	76.9	0.019	0.004
5FeVTi	V	51.4	0.061	0.014
2.5VTi	V	73.7	0.089	0.023
1FeVAl	V	57.7	0.015	0.003
5FeVAl	V	41.9	0.054	0.010
2.5VAl	V	74.7	0.098	0.018
1FeVSi	V	83.4	0.111	0.004
5FeVSi	V	57.3	0.348	0.014
2.5VSi	V	95.9	0.618	0.029

[a] As obtained after 5 days of operation in a stream of nitrogen with 10% oxygen and 10% methanol at 300 °C (see Section 2.3).

alysts, one difficulty is that the true coverage of the support is not known. Moreover, the coverage as well as the catalyst composition, weight and surface area change during the treatment. Except for the coverage, the same changes are also relevant for the bulk samples used as references. Therefore, to give a better picture of the catalysts, in Table 4 the loss of active element is expressed in alternative units, namely relative total amount of active metal in the freshly loaded catalyst (loss %) and per unit mass and unit surface area of the fresh catalyst, respectively. For the supported catalysts any change of total weight or surface area during the treatment should be negligible, considering that the load of active metal is low (Table 1).

Compared with the volatilization of Mo from the industrial-type iron molybdate catalyst, for comparable conditions the data given in Table 4 show that the volatility of V from the $FeVO_4$ bulk sample is considerably lower in spite of the latter phase per unit surface area being twice as active as the molybdate catalyst for methanol oxidation [20]. For the supported catalysts with both vanadium and iron, the relative loss percentage of vanadium is lower for the 5FeV samples than for the 1FeV samples, whereas the loss is higher when expressed as either per unit weight or unit surface area of the fresh catalyst. The decrease of loss percentage with increase of load reflects the formation of some bulk vanadia at the higher load. The formation of bulk vanadia phases, amorphous and crystalline, has been reported in the literature for loads exceeding the monolayer capacity [34,56,57]. However, except for the silica-supported samples, formation of any crystalline bulk vanadia could not be detected by XRD in 5FeVTi and 5FeVAl (Fig. 1) since the vanadium content in these samples is low due to the low surface area of the supports. The fact that the V-loss per unit weight or surface area increases with the load of vanadium and iron is mainly a consequence of an increase in the content and coverage of the support with vanadium. Compared with the TiO_2- and α-Al_2O_3-supported catalysts, those on SiO_2 show larger V-loss both in percentage and per catalyst weight, whereas the values per unit surface area of the support are of similar magnitude. The latter fact is a consequence of the coverage of the SiO_2 support with vanadate being low in agreement with previous comparisons of vanadia on the different supports [13,57]. In the present FeVSi catalysts, XRD (Fig. 1) and XPS (Table 2) show the formation of $FeVO_4$ and some dispersed vanadia species, respectively. Compared with the $FeVO_4$ bulk sample, the considerably higher loss percentage of vanadium from the 5FeVSi sample reflects both the smaller crystallite size of the $FeVO_4$ on SiO_2 and that the dispersed species are only weakly interacting with the silica, which is shown by the relatively large decrease of the V/Si ratio that is notable already after the first 16 h in methanol oxidation (Table 2).

Comparing the data given in Table 4 for the supported 5FeV samples with the data for the corresponding 2.5V samples with the same load of vanadium, it is seen that the presence of Fe has a stabilizing effect on V despite the dispersion of Fe on the former catalysts being lower than that of V (Table 2). Particularly, the volatility expressed per unit surface area of catalyst is lower by a factor 2 for the 5FeV samples, which cannot be explained by any difference in the surface concentration of V as determined by XPS (Table 2). However, regardless of the stabilization of V caused by Fe, the measured loss percentages indicate that neither supported V-oxide nor Fe–V-oxide is of interest for use as a catalyst for methanol oxidation on an industrial scale.

4. Conclusions

Fe–V-oxide (0.5 to 5 theoretical layers) and V-oxide (2.5 theoretical layers) supported on low surface area anatase TiO_2 (4.5 m^2/g), α-Al_2O_3 (4.8 m^2/g) and SiO_2 (25 m^2/g) are active for methanol oxidation. With regard to the type of support, the activity of the supported vanadia decreases in the order $TiO_2 > Al_2O_3 > SiO_2$ in line with the trend shown by XPS data that the surface concentration of V decreases in the same order. Considering both activity and selectivity to formaldehyde, the most interesting catalysts on each support are those with the highest load of vanadium. At 80% methanol conversion, these samples show a selectivity to formaldehyde in the range 80% to 88%, a value which decreases in the order $(Fe)VO_x/TiO_2 \approx (Fe)VO_x/Al_2O_3 > FeVO_x/SiO_2 > VO_x/SiO_2$. Compared with the supported catalysts, the neat $FeVO_4$ is slightly more selective (90%) at the same conditions. In general, for the supported catalysts the effect of iron on the catalytic performance is minor, which is in agreement with XPS analysis showing that V is considerably better dispersed than Fe. The low dispersion of Fe is confirmed by XANES, indicating the formation of α-Fe_2O_3 on TiO_2 and α-Al_2O_3, whereas on SiO_2 both $FeVO_4$ and α-Fe_2O_3 are present.

As revealed by XRD analysis, the low dispersion of active material on silica is due to crystalline $FeVO_4$ and V_2O_5 forms in the presence and absence of iron in the catalyst, respectively. On titania and alumina, besides the support, XRD shows no additional crystalline phases. XANES analysis of fresh samples at ambient conditions shows the presence of both octahedrally (70%) and tetrahedrally (30%) coordinated vanadia species on titania, whereas on alumina and silica the vanadium is essentially tetrahedrally coordinated. Consideration of XANES, XPS and activity data indicates that the alumina is not inert and an $Al_{1-x}Fe_xVO_4$-type structure forms on the surface. XANES confirms that in all fresh samples the deposited metals are in their highest oxidation state,

i.e. V^{5+} and Fe^{3+}. For samples being used for 16 h in methanol oxidation, XANES reveals no major change of structure or oxidation state, except for some reduction of the vanadium on titania forming rutile-type $V_xTi_{1-x}O_2$ with V^{4+}. No simultaneous reduction of iron is noticed. Moreover, XPS shows some reduction of vanadium on silica.

Compared with the volatility of Mo from a commercial-type iron molybdate bulk catalyst, the pure $FeVO_4$ presents considerably lower volatility of V. For the supported (Fe)–V-oxide, the volatilization of V is severer considering the limited vanadium content on the support. After operation at 300 °C for 5 days in methanol oxidation with an approximately constant composition of 10 vol.% each of methanol and oxygen, depending on the load of vanadium and iron not less than about 40% to 80% of the total amount of vanadium in the TiO_2 and Al_2O_3 supported catalysts has volatilized. For the silica supported samples, the volatilization is even worse. Thus, an important conclusion from our work is that supported vanadia hardly is an alternative to either bulk vanadate or bulk molybdate for use as a catalyst in industrial production of formaldehyde by methanol oxidation.

Acknowledgments

The Swedish Research Council (VR) is acknowledged for financial support. Parts of the research were carried out at beamline I811, MAX-lab synchrotron radiation source, Lund University, Sweden. Funding for the beamline I811 project was kindly provided by The Swedish Research Council and The Knut and Alice Wallenberg Foundation.

References

[1] G. Reuss, W. Disteldorf, A.O. Gamer, A. Hilt, Ullmann's Encyclopedia of Industrial Chemistry, seventh ed., vol. A11, Wiley-VCH, Weinheim, 2008, pp. 619–652.
[2] B. Crichton, in: Informally Speaking (newsletter from Perstorp Formox, <www.perstorpformox.com>), spring/summer 2003, pp. 12–13.
[3] Methanex Corporation, Vancouver, Canada (methanol prices from 2002 to 2008, <www.methanex.com>).
[4] N. Burriesci, F. Garbassi, M. Petrera, G. Petrini, N. Pernicone, in: B. Delmon, G.F. Froment (Eds.), Catalyst Deactivation, Elsevier, Amsterdam, 1980, pp. 115–126.
[5] A.P.V. Soares, M.F. Portela, A. Kiennemann, J.M.M. Millet, React. Kinet. Catal. Lett. 75 (2002) 13.
[6] A.P.V. Soares, M.F. Portela, A. Kiennemann, L. Hilaire, Chem. Eng. Sci. 58 (2003) 1315.
[7] A. Andersson, M. Hernelind, O. Augustsson, Catal. Today 112 (2006) 40.
[8] B.I. Popov, V.N. Bibin, G.K. Boreskov, Kinet. Katal. (Eng. Transl.) 17 (1976) 322.
[9] P. Forzatti, E. Tronconi, A.S. Elmi, G. Busca, Appl. Catal. A 157 (1997) 387.
[10] R. Maliński, React. Kinet. Catal. Lett. 5 (1976) 265.
[11] R. Maliński, M. Akimoto, E. Echigoya, J. Catal. 44 (1976) 101.
[12] G. Deo, I.E. Wachs, J. Haber, Crit. Rev. Surf. Chem. 4 (1994) 141.
[13] G. Deo, I.E. Wachs, J. Catal. 146 (1994) 323.
[14] S. Lim, G.L. Haller, Appl. Catal. A 188 (1999) 277.
[15] X. Gao, I.E. Wachs, Top. Catal. 18 (2002) 243.
[16] L.E. Briand, J-M. Jehng, L. Cornaglia, A.M. Hirt, I.E. Wachs, Catal. Today 78 (2003) 257.
[17] G.V. Isaguliants, I.P. Belomestnykh, Catal. Today 100 (2005) 441.
[18] I.E. Wachs, L.E. Briand, US Patent 7 193 117 B2, Lehigh University, 2007.
[19] T. Kim, I.E. Wachs, J. Catal. 255 (2008) 197.
[20] R. Häggblad, J.B. Wagner, S. Hansen, A. Andersson, J. Catal. 258 (2008) 345.
[21] H. Zhang, Z. Liu, Z. Feng, C. Li, J. Catal. 260 (2008) 295.
[22] P.-O. Larsson, A. Andersson, L.R. Wallenberg, B. Svensson, J. Catal. 163 (1996) 279.
[23] JCPDS International Centre for Diffraction data, Powder Diffraction File, Swarthmore, PA, 1991.
[24] R.A. Spurr, H. Myers, Anal. Chem. 29 (1957) 760.
[25] G.C. Bond, A.J. Sárkány, G.D. Parfitt, J. Catal. 57 (1979) 476.
[26] J.P. Balikdjian, A. Davidson, S. Launay, H. Eckert, M. Che, J. Phys. Chem. B 104 (2000) 8931.
[27] J. Papachryssanthou, E. Bordes, A. Vejux, P. Courtine, R. Marchand, M. Tournoux, Catal. Today 1 (1987) 219.
[28] S.T. Martin, C.L. Morrison, M.R. Hoffmann, J. Phys. Chem. 98 (1994) 13695.
[29] L.E. Depero, P. Bonzi, M. Musci, C. Casale, J. Solid State Chem. 111 (1994) 247.
[30] S.L.T. Andersson, S. Järås, J. Catal. 64 (1980) 51.
[31] L. O'Mahony, T. Curtin, D. Zemlyanov, M. Mihov, B.K. Hodnett, J. Catal. 227 (2004) 270.
[32] E. Baba Ali, J.C. Bernède, A. Barreau, Mater. Chem. Phys. 63 (2000) 208.
[33] K. Asami, K. Hashimoto, Corros. Sci. 17 (1977) 559.
[34] G.C. Bond, J.C. Védrine, Catal. Today 20 (1994) 171.
[35] B.M. Weckhuysen, D.E. Keller, Catal. Today 78 (2003) 25.
[36] K. Inumaru, M. Misono, T. Okuhara, Appl. Catal. A 149 (1997) 133.
[37] I.E. Wachs, B.M. Weckhuysen, Appl. Catal. A 157 (1997) 67.
[38] N.U. Zhanpeisov, Res. Chem. Intermed. 30 (2004) 133.
[39] I.E. Wachs, J. Catal. 124 (1990) 570.
[40] H. Eckert, I.E. Wachs, J. Phys. Chem. 93 (1989) 6796.
[41] O.B. Lapina, A.A. Shubin, A.V. Nosov, E. Bosch, J. Spengler, H. Knözinger, J. Phys. Chem. B 103 (1999) 7599.
[42] U.G. Nielsen, N.-Y. Topsøe, M. Brorson, J. Skibsted, H.J. Jakobsen, J. Am. Chem. Soc. 126 (2004) 4926.
[43] T. Tanaka, H. Yamashita, R. Tsuchitani, T. Funabiki, S. Yoshida, J. Chem. Soc., Faraday Trans. I 84 (1988) 2987.
[44] J. Holmberg, R. Häggblad, A. Andersson, J. Catal. 243 (2006) 350.
[45] E. Arisi, S.A. Palomares Sánchez, F. Leccabue, B.E. Watts, G. Bocelli, F. Calderón, G. Calestani, L. Righi, J. Mater. Sci. 39 (2004) 2107.
[46] S. Yoshida, T. Tanaka, Y. Nishimura, H. Hizutani, T. Funabiki, in: M.J. Phillips, M. Ternan (Eds.), Proceedings of the 9th International Congress on Catal., vol. 3, The Chemical Institute of Canada, Ottawa, 1988, pp. 1473–1480.
[47] M. Ruitenbeek, A.J. van Dillen, F.M.F. de Groot, I.E. Wachs, J.W. Geus, D.C. Koningsberger, Top. Catal. 10 (2000) 241.
[48] H.G. Bütter, G.J. Kearley, C.J. Howard, F. Fillaux, Acta Cryst. B 50 (1994) 435.
[49] J.M. Tatibouët, Bull. Soc. Chim. France 1 (1986) 18.
[50] J.-M. Jehng, G. Deo, B.M. Weckhuysen, I.E. Wachs, J. Mol. Catal. A 110 (1996) 41.
[51] S. Takenaka, T. Tanaka, T. Yamazaki, T. Funabiki, S. Yoshida, J. Phys. Chem. B 101 (1997) 9035.
[52] J.N.J. van Lingen, O.L.J. Gijzeman, B.M. Weckhuysen, J.H. van Lenthe, J. Catal. 239 (2006) 34.
[53] D.E. Keller, S.M.K. Airaksinen, A.O. Krause, B.M. Weckhuysen, D.C. Koningsberger, J. Am. Chem. Soc. 129 (2007) 3189.
[54] M. Cavalleri, K. Hermann, A. Knop-Gericke, M. Hävecker, R. Herbert, C. Hess, A. Oestereich, J. Döbler, R. Schlögl, J. Catal. 262 (2009) 215.
[55] F. Roozeboom, P.D. Cordingley, P.J. Gellings, J. Catal. 68 (1981) 464.
[56] B. Grzybowska-Świerkosz, Appl. Catal. A 157 (1997) 263.
[57] H. Tian, E.I. Ross, I.E. Wachs, J. Phys. Chem. B 110 (2006) 9593.